

# Numerical calculation of Z-scan measurements for non-linear media with large phase shift

M. D. Zidan\* and A. Allahham

*Department of Physics, Atomic Energy Commission of Syria, P. O. Box 6091, Damascus, Syria*

(Received 4 July 2023; Revised 6 August 2023)

©Tianjin University of Technology 2024

We have reported the characteristics of a Z-scan for the poly(azaneylylidene-acylene) (DAZA) polymer, as nonlinear medium with a large nonlinear phase shift using continuous-wave (CW) laser beam. It has been verified that the Fresnel diffraction model is applicable for analyses of Z-scan measurements with DAZA polymer at high laser power. It was found that Z-scan curves with peak-to-valley features appear as the applied light intensity increases in the case of a large nonlinear phase shift. The Z-scan experiments were carried out using a CW laser to verify the theoretical calculations in the case of a large nonlinear phase shift model. Our results show good agreements between the experimental data and the proposed theoretical models.

**Document code:** A **Article ID:** 1673-1905(2024)03-0177-6

**DOI** <https://doi.org/10.1007/s11801-024-3123-4>

Nonlinear optical (NLO) effects would be induced as result of interaction between high power laser beam and matter (medium)<sup>[1]</sup>. These nonlinear effects can cause observable changes in the NLO properties of the studied medium<sup>[2]</sup>. The nonlinear refraction index ( $n_2$ ) and nonlinear absorption ( $\beta$ ) are the most important parameters required to determine the real and imaginary parts of the third order NLO susceptibility  $\chi^3$  of different new molecules<sup>[3,4]</sup>.

Determining the NLO response of new prepared compounds will assess the type of future photonic devices<sup>[5]</sup>. The Z-scan technique, developed by SHEIK-BAHAE et al<sup>[6,7]</sup> was considered as very effective tool, simple, sensitive and most reliable for determining the changes of sign and magnitudes in nonlinear refractive index and nonlinear absorption<sup>[8,9]</sup>. It was utilized to investigate a large number of materials, such as TiO<sub>2</sub> nanoparticles on graphene oxide<sup>[10]</sup>, Zn<sub>3</sub>Mo<sub>2</sub>O<sub>9</sub> nanosheet ceramic material<sup>[11]</sup>, hybrid organic-inorganic materials<sup>[12-14]</sup>, organic dyes<sup>[15,16]</sup> and MXene Ti<sub>3</sub>C<sub>2</sub>T<sub>x</sub> flakes over the spectral range from 800 nm to 1 800 nm<sup>[17]</sup>. Usually, in the Z-scan technique, the transmittance is measured as function of the sample position Z with respect to the focal point ( $Z=0$ ). In the case of closed aperture configuration, the transmittance is a peak-valley curve, which indicates to negative nonlinear response and valley-peak curve for positive nonlinear response<sup>[7]</sup>.

The proposed theoretical model by SHEIK-BAHAE (SBM) is only valid for the local nonlinear media, it cannot be applied for the nonlocal nonlinear media<sup>[18]</sup>. However, different theoretical models can be applied in

order to perform best fitting to the new experimental curves of nonlocal nonlinear media<sup>[19]</sup>.

This article presents a new experimental and theoretical study of poly(azaneylylidene-acylene) (DAZA) polymer using closed Z-scan technique. Different theoretical models were used to perform suitable fitting of the experimental data with large phase changes and nonlocal response in the presence of nonlinear refraction.

Preparation and characterization of DAZA polymer was described elsewhere<sup>[20]</sup>. DAZA polymer has good mechanical properties, high chemical stability, thermal stability, UV-visible spectral range, and exhibit fast NLO response time. The DAZA polymer was dissolved in chloroform with concentration of 10<sup>-3</sup> M. The closed Z-scan measurements were acquired with similar experimental setup, which was mentioned in Ref.[21]. A continuous-wave (CW) diode pumped solid state laser is used with  $\lambda=532$  nm and the power up to 100 mW. A special optical filter was inserted in front of the laser beam to get very good high quality TEM<sub>00</sub> Gaussian beam. The laser beam is focused onto the cell samples (2 mm thickness) using positive lens with 10 cm focal length. The spot size in the focal region was 47  $\mu$ m and the transmittance intensity was recorded by means of power meter. All the components of the experiment were fully controlled by computer.

The value of nonlinear refractive index ( $n_2$ ) of the DAZA polymer was determined using the closed aperture Z-scan configuration. The sample cell was gradually moved along the axis of propagation (Z-axis) of a focused Gaussian laser beam. Acquisition of the experimental data was performed by the recording of the

---

\*E-mail: mdzidan@aec.org.sy

transmission output of the sample cell. As the sample experiences different intensities at different positions, the recording of transmission as a function of Z-coordinate provides accurate information about the presence of non-linear effect. All the acquired results of studying the DAZA polymer are presented in Figs.1—4. These results show the normalized transmittance of closed Z-scan measurements as a function of distance from the focal point (Z=0) with different laser power of 0.6 mW, 1 mW, 2 mW, 4 mW, 6 mW and 8 mW. Then, we have applied suitable theoretical models in order to get the best fitting of the experimental data for each case. Fig.1 presents the closed aperture Z-scan data at laser power of 0.6 mW. Then, the SBM and thermal lens model (TLM) have been used as theoretical models to perform the fitting processes<sup>[7]</sup>. The solid curve depicted in Fig.1(a) was obtained from fitting by SBM in Eq.(1), which represents the closed aperture Z-scan normalized transmittance<sup>[22]</sup>.

$$T(Z, \Delta\phi_0) = 1 - \frac{4 \Delta\phi_0 X}{(X^2 + 9)(X^2 + 1)}, \quad (1)$$

where is  $X=(Z/Z_0)$ , and  $T$  is the normalized transmittance for the pure  $n_2$ , and  $\Delta\phi_0$  is the on-axis small nonlinear phase shift change. Then, the TLM (Cuppo's equation)<sup>[18]</sup> was applied to get the best fitting for the same experimental data. The solid curve depicted in Fig.1(b) was obtained using the TLM (Cuppo's equation), and the normalized transmittance for closed aperture Z-scan is given in<sup>[23]</sup>

$$T(z) = \left( 1 + \frac{\frac{2Z}{Z_0}}{1 + \left(\frac{Z}{Z_0}\right)^2} \theta + \frac{1}{1 + \left(\frac{Z}{Z_0}\right)^2} \theta^2 \right)^{-1}, \quad (2)$$

where  $\theta$  is the on-axis phase shift ( $\theta = \frac{(dn/dT) \alpha P L_{\text{eff}}}{\lambda k}$ ),  $\alpha$

is the absorption coefficient of the sample,  $L_{\text{eff}}$  is the sample effective length,  $(dn/dT)$  is the thermo-optic coefficient, and  $P$  is the laser power.

It can be seen that there is slight deviation between the theoretical curve of SBM and the experimental data. But, it is very good agreements between the thermal lens model curves generated by TLM and the experimental data. The observed asymmetric feature of the closed Z-scan data, using CW laser beam, suggests that the origin of the nonlinear refractive index ( $n_2$ ) is thermo-optic<sup>[8]</sup>. The experimental parameters for the closed Z-scan can be used with the two models of SBM and TLM in order to calculate the  $n_2^{\text{th}}$  and  $dn/dT$ , and all the obtained values of  $n_2$  were listed in Tab.1.

The closed Z-scan data were taken at two laser power levels of 1 mW and 2 mW, as seen in Fig.2. The features of the curves in Fig.2 are asymmetric, by applying the SBM to the experimental data, it was found not suitable to be used as theoretical model to extract the experimental parameters.

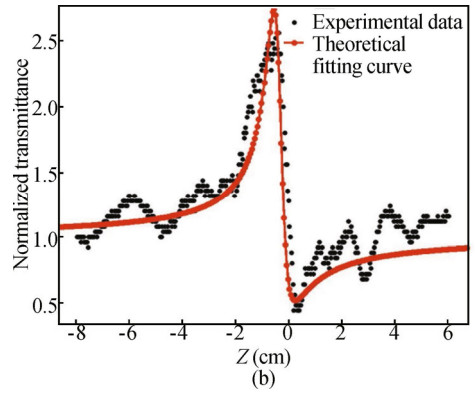
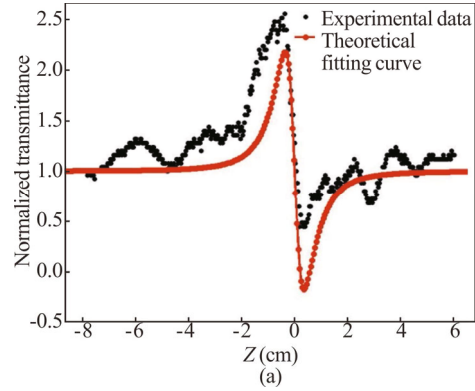


**Fig.1** Closed aperture Z-scan data for DAZA polymer at the laser power of 0.6 mW using (a) SBM and (b) TLM

**Tab.1** Calculated values of thermal nonlinear refractive index ( $n_2^{\text{th}}$ ) and thermo-optic coefficients ( $dn/dT$ ) at 0.6 mW

Theoretical model	$n_2^{\text{th}}$ (cm <sup>2</sup> /W)	$dn/dT$ (K <sup>-1</sup> )
SBM	$7.06 \times 10^{-7}$	$2.49 \times 10^{-4}$
TLM	$7.02 \times 10^{-7}$	$1.89 \times 10^{-4}$

Then, the TLM has been applied for getting the best fitting of the experimental data using Eq.(2). The solid curves depicted in Fig.2(a) and (c) were obtained by utilizing Eq.(2) with two input laser power levels of 1 mW and 2 mW. As the applied power increases, the thermal phase shift becomes larger, and the SBM may not be a valid assumption for calculating the phase shift or the nonlinear refractive index ( $n_2$ ). The aberrant thermal lens model (ATLM) was used to perform the fitting of the recorded experimental data at two laser power levels of 1 mW and 2 mW using<sup>[24,25]</sup>

$$T(Z) = \left[ 1 + \frac{\theta}{2} \tan^{-1} \left( \frac{\frac{2Z}{Z_0}}{3 + \left(\frac{Z}{Z_0}\right)^2} \right) \right] + \left[ \frac{\theta}{4} \ln \left( \frac{1 + \left(\frac{Z}{Z_0}\right)^2}{9 + \left(\frac{Z}{Z_0}\right)^2} \right) \right]^2. \quad (3)$$

The solid curves of Fig.2(b) and (d) indicated to the fitting results of using Eq.(3) at two input laser power

levels of 1 mW and 2 mW. Looking to the present results, it is found slight deviation between the experimental data and the theoretical curve of the ATLM. The experimental results agree with the predicted results obtained by the theoretical of TLM using Eq.(2). Therefore, the TLM under CW laser reported by CUPPO *et al*<sup>[18]</sup> was used for predication of the correct values of  $n_2$ , the thermo-optic coefficients  $dn/dT$  and  $\theta$  coefficients. At the same time, the values of  $n_2$ ,  $dn/dT$  and  $\theta$  were calculated using the TLM and the ATLM at 1 mW and 2 mW, and all the obtained values were listed in Tab.2.

Then, the closed Z-scan measurements were taken at higher laser power equal up to 4 mW and 6 mW, as seen in Fig.3. The TLM (Eq.(2)) and ATLM (Eq.(3)) have been used to perform the best fitting of the experimental data. As clearly seen in curves of Fig.3(a)—(c), the experimental data was in excellent agreement with the

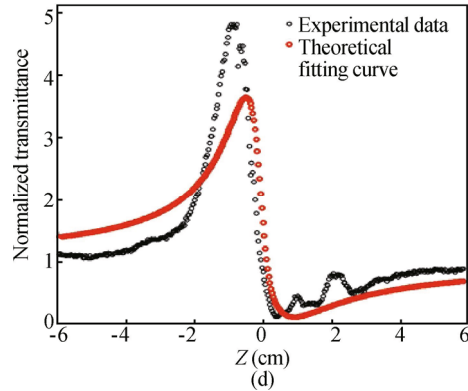
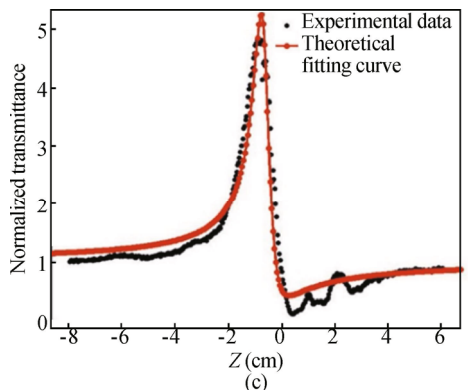
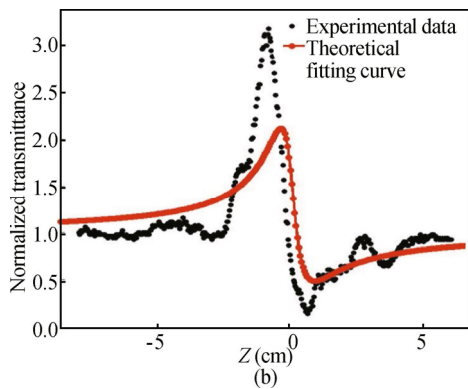
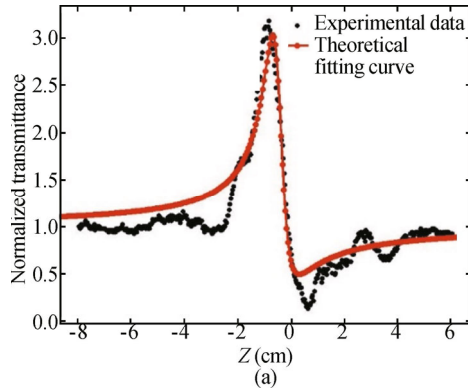


**Fig.2 Closed aperture Z-scan data for DAZA polymer at the two laser power levels of 1 mW and 2 mW using (a) TLM (1 mW), (b) ATLM (1 mW), (c) TLM (2 mW), and (d) ATLM (2 mW)**

**Tab.2 Calculated values of thermal nonlinear refractive index ( $n_2^{th}$ ) and thermo-optic coefficients ( $dn/dT$ ) at the two laser power levels of 1 mW and 2 mW**

Theoretical model	Laser Power	$n_2^{th}$ (cm <sup>2</sup> /W)	$dn/dT$ (K <sup>-1</sup> )	$\theta$
ATLM	1 mW	$8.27 \times 10^{-7}$	$2.23 \times 10^{-4}$	1.441
	2 mW	$6.29 \times 10^{-7}$	$1.96 \times 10^{-4}$	2.191
TLM	1 mW	$4.48 \times 10^{-7}$	$1.21 \times 10^{-4}$	0.78
	2 mW	$2.78 \times 10^{-7}$	$7.49 \times 10^{-5}$	0.969



TLM theoretical prediction. But, there are slight deviations between the experimental data and the theoretical curves of using ATLM, as seen in Fig.3(b)—(d). Using the output results of two theoretical models (ATLM and TLM) at two laser power levels of 4 mW and 6 mW, we were able to calculate the values of the thermal nonlinear refractive index  $n_2^{th}$ , the thermo-optic  $dn/dT$  and  $\theta$  coefficients of DAZA polymer at 4 mW and 6 mW and they are inserted in Tab.3.

Finally, the closed Z-scan measurements of DAZA polymer were taken at higher laser power equal to 8 mW (Fig.4). Then, three theoretical models were used to search for the best theoretical model for fitting of the experimental data. The solid curves in Fig.4(a) and (b) were obtained by the mentioned TLM, ATLM using Eqs.(2) and (3), respectively. The solid curve in Fig.4(c) was obtained from the best fitting by numerically solving the integrals in Eq.(4) (Fresnel diffraction model) as the sample is considered as thin sample and no absorption, and the normalized transmittance at the aperture can be determined with the following equation<sup>[26,27]</sup>

$$T(Z, \Delta\phi_0, a) = \frac{\int_0^a \int_0^a j_0 \left( k \frac{\rho}{D-Z} r \right) \exp \left( -\frac{r^2}{\omega^2(Z)} - i\phi(Z, r) \right) r dr \Big|_{\rho=d\rho}}{\int_0^a \int_0^a j_0 \left( k \frac{\rho}{D-Z} r \right) \exp \left( -\frac{r^2}{\omega^2(Z)} - i \frac{kr^2}{2R(Z)} \right) r dr \Big|_{\rho=d\rho}}, \quad (4)$$

where  $\phi(Z,r) = \frac{k r^2}{2R(Z)} + \Delta\phi(Z,r)$ ,  $\rho=(D-Z)\theta$  is the radial coordinate on the aperture plane at distance  $D$ ,  $\theta$  is

the far-field diffraction angle,  $a$  is the aperture radius, and all the others terms in the Eq.(4) were defined in Ref.[28].

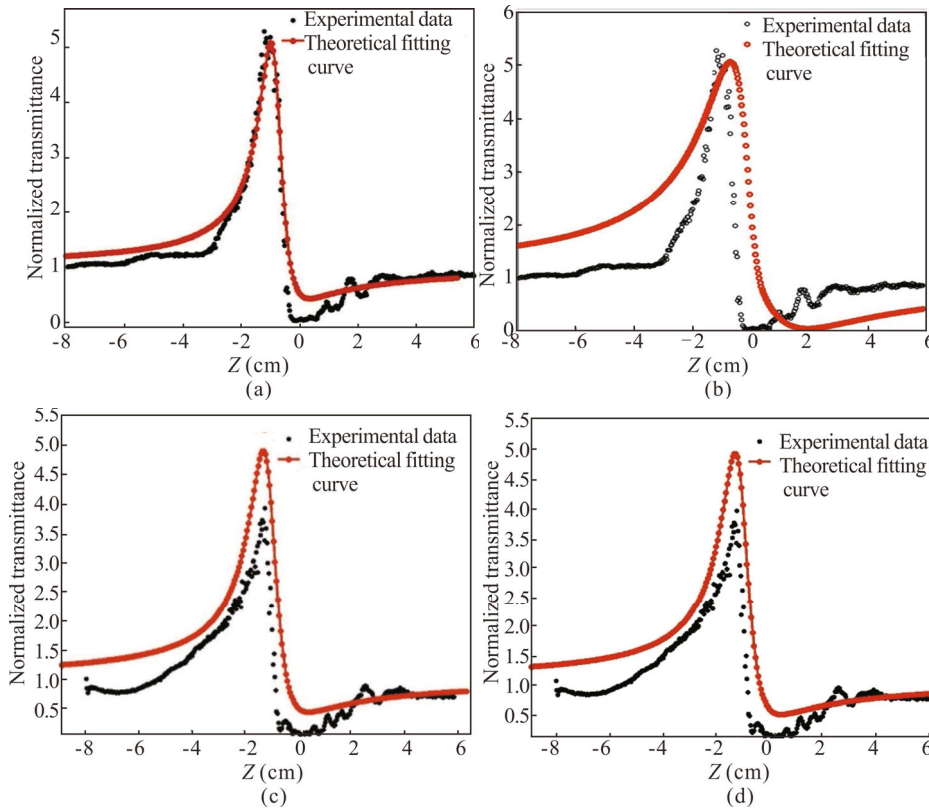


**Fig.3** Closed aperture Z-scan data for DAZA polymer at the two laser power levels of 4 mW and 6 mW using (a) TLM (4 mW), (b) ATLM (4 mW), (c) TLM (6 mW), and (d) ATLM (6 mW)

**Tab.3** Calculated values of thermal nonlinear refractive index ( $n^{th}_2$ ) and thermo-optic coefficients ( $dn/dT$ ) at the two laser power levels of 4 mW and 6 mW

Theoretical model		$n^{th}_2$ (cm <sup>2</sup> /W)	$dn/dT$ (K <sup>-1</sup> )	$\theta$
ATLM	4 mW	$3.88 \times 10^{-7}$	$1.04 \times 10^{-4}$	2.70
	6 mW	$3.06 \times 10^{-7}$	$8.24 \times 10^{-4}$	3.20
TLM	4 mW	$1.38 \times 10^{-7}$	$3.71 \times 10^{-5}$	0.960
	6 mW	$9.18 \times 10^{-8}$	$2.47 \times 10^{-5}$	0.959

As it is clearly shown in Fig.4, the experimental results of DAZA polymer for closed Z-scan measurements do not agree with the two applied models TLM and ATLM. There are slight deviations between the experimental data and the theoretical curves. An excellent fitting can be obtained with the Fresnel diffraction model (Eq.(4)). However, the mentioned analytical formula (ATLM and TLM) of the on-axis transmission for determining the nonlinear index of refraction of materials were not suitable, for large nonlinear phase shifts materials. So, it is possible to consider such model like the diffraction model to be used in large

phase shifts materials in Z-scan experiments. A noticeable asymmetry around the origin has been developed on the normal transmittance curves for large values of the nonlinear phase shift. This asymmetry becomes more pronounced with larger values of the nonlinear phase shift, for  $\Delta\phi_0$  values equal to (or greater than)  $2\pi^{[26]}$ . The experimental results of DAZA polymer at 8 mW using three theoretical models for large thermal phase shift were used to extract the fitting parameters, such as the thermal nonlinear refractive index  $n^{th}_2$ , and thermo-optic coefficients  $dn/dT$  using the following relations<sup>[29]</sup>



$$n_2^{\text{th}} = \frac{\theta}{I_0 k L_{\text{eff}}}, \quad (5)$$

$$\frac{dn}{dT} = \frac{\lambda k}{\alpha P L_{\text{eff}}} \theta, \quad (6)$$

where  $I_0$  is the on-axis irradiance at focus. All the obtained values are tabulated in Tab.4.

Finally, it can be said that our new experimental results on DAZA polymer were agreed with the theoretical models at higher laser power, as well as these results are well agreed with the results of similar pervious reported work<sup>[19,25]</sup>.

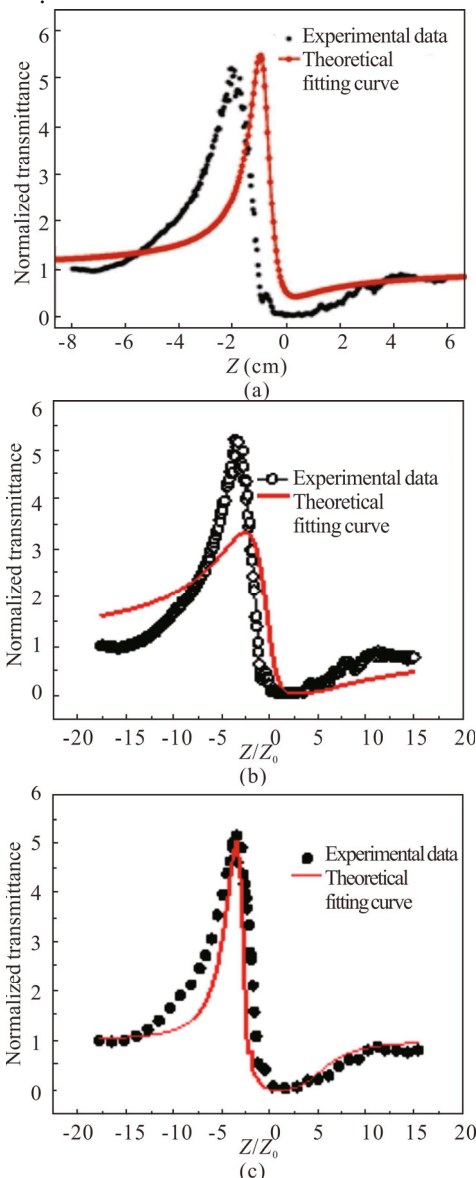


**Fig.4 Closed aperture Z-scan data for DAZA polymer at the laser power level of 8 mW using (a) TLM, (b) ATLM, and (c) diffraction model**

We present the results of Z-scan experimental and numerical investigation of DAZA polymer. The closed Z-scan measurement of DAZA polymer exhibits an asymmetric behavior due to the nonlocal thermal nonlinear refraction. A theoretical analysis based on the

**Tab.4 Calculated values of thermal nonlinear refractive index ( $n_2^{\text{th}}$ ), thermo-optic coefficients ( $dn/dT$ ) and  $\theta$  coefficients at the laser power level of 8 mW**

Theoretical model	$n_2^{\text{th}}$ (cm <sup>2</sup> /W)	$dn/dT$ (K <sup>-1</sup> )	$\theta$
TLM	$6.76 \times 10^{-8}$	$1.80 \times 10^{-5}$	0.942
ATLM	$3.06 \times 10^{-7}$	$8.24 \times 10^{-4}$	0.780
Fresnel diffraction model	$3.01 \times 10^{-7}$	$8.11 \times 10^{-5}$	4.20

SBM, TLM and ATLM shows slight deviations from the experimental closed Z-scan results for the DAZA polymer at different input laser power levels. Our results have shown that the Fresnel diffraction model is the best model to be used for large nonlinear phase shift induced in the DAZA polymer. The new results are found to be in excellent agreement with this analysis and the values of the nonlinear refractive index and thermo-optic coefficients are extracted and calculated using the mentioned theoretical models.

**Acknowledgements**

The authors would like to thank Prof. I. Othman, Director General of AECS and Prof. M. K. Sabra for their support.

**Ethics declarations**

**Conflicts of interest**

The authors declare no conflict of interest.

**References**

- [1] RAMÍREZ-MARTÍNEZ D, ALVARADO-MÉNDEZ E, TREJO-DURÁN M, et al. Nonlocal nonlinear refraction in Hibiscus sabdariffa with large phase shifts[J]. Optics express, 2014, 22: 25161-25170.
- [2] YADAV S B, TAWARE S, SREENATH M C, et al. Experimental and theoretical investigation of linear and nonlinear optical properties of ethyl-3-hydroxy-2-naphthoate azo dyes by solvatochromic, computational aspects, and Z-scan technique[J]. Journal of physical organic chemistry, 2020, 33: e4050.
- [3] JEYARAM S, HEMALATHA S, GEETHAKRISHNAN T. Nonlinear refraction, absorption and optical limiting properties of disperse blue 14 dye[J]. Chemical physics letters, 2020, 739: 137037.
- [4] CHOUBEY R, MEDHEKAR S, KUMAR R, et al. Study of nonlinear optical properties of organic dye by Z-scan technique using He-Ne laser[J]. Journal of materials science: materials in electronics, 2014, 25: 1410-1415.
- [5] BINISH B, RAHULAN K M, HEGDE T A, et al. Enhanced third order non-linear optical characteristics of Ba<sup>2+</sup> doped CoMoO<sub>4</sub> nanostructures[J]. Optical materials, 2022, 131: 112694.
- [6] SHEIK-BAHAE M, SAID A A, VAN STRYLAND E W. High-sensitivity, single-beam n<sub>2</sub> measurements[J].

- Optics letters, 1989, 14: 955-957.
- [7] SHEIK-BAHAIE M, SAID A A, WEI T H, et al. Sensitive measurement of optical nonlinearities using a single beam[J]. IEEE journal of quantum electronics, 1990, 26: 760.
- [8] ZIDAN M D, ALLAF A W, ALLAHHAM A, et al. Investigation of nonlinear optical properties of chromium tetrapyrrole dicarbonyl complex[J]. Optik, 2020, 200: 163175.
- [9] ZIDAN M D, AL-KTAIFANI M M, EL-DAHER M S, et al. Diffraction ring patterns and nonlinear measurements of the Tris(2',2-bipyridyl)iron(II) tetrafluoroborate[J]. Optics & laser technology, 2020, 131: 106449.
- [10] GAWAS P, NUTALAPATI V, NARAYANARAO D, et al. Broadband optical power limiting with the decoration of TiO<sub>2</sub> nanoparticles on graphene oxide[J]. Optical materials, 2020, 109: 110366.
- [11] ZHANG K, HE J, SHEN R, et al. Synthesis and tunable nonlinear absorption properties of Zn<sub>3</sub>Mo<sub>2</sub>O<sub>9</sub> nanosheet ceramic material[J]. Optical materials, 2020, 99: 109570.
- [12] ZIDAN M D, AL-KTAIFANI M M, EL-DAHER M S, et al. Synthesis and nonlinear optical study of the hybrid salt: [C<sub>12</sub>H<sub>14</sub>N<sub>2</sub>][Fe(CN)<sub>5</sub>(NO)]·5H<sub>2</sub>O[J]. Journal of nonlinear optical physics & materials, 2022, 31: 2250015.
- [13] YUAN Y, ZHOU W, ZHU Y, et al. Synthesis, characterization and third-order nonlinear optical behaviour of two novel ethyne-linked polymers[J]. Dyes and pigments, 2022, 204: 110423.
- [14] ZIDAN M D, AL-KTAIFANI M M, ALLAHHAM A, et al. Nonlinear optical investigation of the Tris(2',2-bipyridyl)iron(II) tetrafluoroborate using z-scan technique[J]. Optics laser technology, 2017, 90: 174-178.
- [15] HASSAN Q M A, RAHEEM N A, EMSHARY C A, et al. Preparation, DFT and optical nonlinear studies of a novel azo-(β)-diketone dye[J]. Optics & laser technology, 2022, 148: 107705.
- [16] HASSAN Q M A, AL-ASADI R H, SULTAN H A, et al. A novel azo compound derived from ethyl-4-amino benzoate: synthesis, nonlinear optical properties and DFT investigations[J]. Optical and quantum electronics, 2023, 55.
- [17] JIANG X, LIU S, LIANG W, et al. Broadband nonlinear photonics in few-layer MXene Ti<sub>3</sub>C<sub>2</sub>T<sub>x</sub> (T=F, O, or OH)[J]. Laser & photonics reviews, 2018, 12: 1700229.
- [18] CUPPO F L S A, FIGUEIREDO N A M, GÓMEZ S L, et al. Thermal-lens model compared with the Sheik-Bahae formalism in interpreting Z-scan experiments on lyotropic liquid crystals[J]. Journal of the optical society of America B, 2002, 19: 1342-1348.
- [19] GARCIA R E V, ARROYO C M L, MENDEZ O M M, et al. Z-scan and spatial self-phase modulation of a Gaussian beam in a thin nonlocal nonlinear media[J]. Journal of optics, 2011, 13: 085203.
- [20] ZIDAN M D, ALLAF A W, ALLAHHAM A, et al. Effect of sample position on formation of spatial-self phase modulation ring patterns in poly(azaneylylidene-acylene)[J]. Optik, 2023, 283: 170939.
- [21] ZIDAN M D, ARFAN A, ALLAHHAM A. Synthesis and nonlinear optical properties of ionic liquids like by Z-scan technique[J]. Revue roumaine de chimie, 2022, 67: 263-270.
- [22] YAO B, REN L, HOU X. Z-scan theory based on a diffraction model[J]. Journal of the optical society of America B, 2003, 20: 1290-1294.
- [23] KARIMZADEH R, ALEALI H, MANSOUR N. Thermal nonlinear refraction properties of Ag<sub>2</sub>S semiconductor nanocrystals with its application as a low power optical limiter[J]. Optics communications, 2011, 284: 2370-2375.
- [24] CARTER C A, HARRIS J M. Comparison of models describing the thermal lens effect[J]. Applied optics, 1984, 23: 476-481.
- [25] SARKHOSH L, MANSOUR N. Analysis of Z-scan measurement for large thermal nonlinear refraction in gold nanoparticle colloid[J]. Journal of nonlinear optical physics & materials, 2015, 24: 1550014.
- [26] RASHIDIAN V M R. Role of the aperture in Z-scan experiments: a parametric study[J]. Chinese physics B, 2015, 24: 114206.
- [27] KOUISHKI E, FARZANEH A, MOUSAVI S H. Closed aperture Z-scan technique using the Fresnel-Kirchhoff diffraction theory for materials with high nonlinear refractions[J]. Applied physics B, 2010, 99: 565-570.
- [28] GHANEM A, ZIDAN M D, EL-DAHER M S. Diffraction ring patterns of the acid blue 29 in different solvents[J]. Results in optics, 2022, 9: 100268.
- [29] SARKHOSH L, ALEALI H, KARIMZADEH R, et al. Large thermally induced nonlinear refraction of gold nanoparticles stabilized by cyclohexanone[J]. Physica status solidi (a), 2010, 207: 2303-2310.